Characterization of Gaussian self-similar stochastic processes using wavelet-based informational tools

L. Zunino*
Centro de Investigaciones Ópticas, casilla de correo 124 Correo Central, 1900 La Plata, Argentina and Departamento de Ciencias Básicas, Facultad de Ingeniería, Universidad Nacional de La Plata (UNLP), 1900 La Plata, Argentina

D. G. Pérez†
Instiuto de Física, Pontificia Universidad Católica de Valparaíso (PUCV), 23-40025 Valparaíso, Chile

M. T. Martín‡ and A. Plastino§
Instituto de Física, Facultad de Ciencias Exactas, Universidad Nacional de La Plata (UNLP), casilla de correo 727, 1900 La Plata, Argentina and Argentina's National Research Council (CONICET), Argentina

M. Garavaglia‖
Centro de Investigaciones Ópticas, casilla de correo 124 Correo Central, 1900 La Plata, Argentina and Departamento de Física, Facultad de Ciencias Exactas, Universidad Nacional de La Plata (UNLP), 1900 La Plata, Argentina

O. A. Rosso¶
Chaos and Biology Group, Instituto de Cálculo, Facultad de Ciencias Exactas y Naturales, Universidad de Buenos Aires (UBA), Pabellón II, Ciudad Universitaria, 1428 Ciudad de Buenos Aires, Argentina

(Received 16 August 2006; published 20 February 2007)

Efficient tools to characterize stochastic processes are discussed. Quantifiers originally proposed within the framework of information theory, like entropy and statistical complexity, are translated into wavelet language, which renders the above quantifiers into tools that exhibit the important "localization" advantages provided by wavelet theory. Two important and popular stochastic processes, fractional Brownian motion and fractional Gaussian noise, are studied using these wavelet-based informational tools. Exact analytical expressions are obtained for the wavelet probability distribution. Finally, numerical simulations are used to validate our analytical results.

DOI: 10.1103/PhysRevE.75.021115 PACS number(s): 02.50.Ey

I. INTRODUCTION

The aim of this paper is to explore the ability of some formerly introduced wavelet-based informational quantifiers to characterize stochastic processes. In that sense, we analyze two well-known stochastic processes, namely, (1) fractional Brownian motion (FBM) and (2) fractional Gaussian noise (FGN) [1,2]. We are mainly interested in Gaussian and self-similar stochastic processes. Gaussian processes are important because they yield the basic model for the analysis of natural phenomena. A process is called Gaussian if all its finite dimensional distributions are Gaussian. Furthermore, considering the ubiquity of Gaussian distributions in probability theory, it is natural to study Gaussian processes. The central limit theorem constitutes a cornerstone of our understanding of the probabilistic nature of the observable world. When there are reasons to suspect the presence of a large number of small perturbations acting both additively and independently, it is reasonable to assume that the concomitant observations will be Gaussian-distributed [3]. That is, if the tails associated to the probability distributions decay fast enough. On the other hand, self-similar stochastic processes are invariant in distribution under suitable scaling of time and space. Formally, a (stochastic) process $X(t)$ is *self-similar* with index H if, for any $c>0$,

$$X(t) \overset{d}{=} c^H X(c^{-1}t), \tag{1}$$

where $\overset{d}{=}$ is equality in distribution. The self-similarity appears in a natural way from limit theorems for sums of random variables [4–6]. Following the arguments mentioned by Beran [7], within the framework of stochastic processes, the role performed by self-similar ones is equivalent to the role of stable distributions among distributions.

*Also at Departamento de Física, Facultad de Ciencias Exactas, Universidad Nacional de La Plata (UNLP). Electronic address: lucianoz@ciop.unlp.edu.ar
†Electronic address: dario.perez@ucv.cl
‡Electronic address: mtmartin@fisica.unlp.edu.ar
§Electronic address: plastino@fisica.unlp.edu.ar
‖Electronic address: garavagliam@ciop.unlp.edu.ar
¶Electronic address: oarosso@fibertel.com.ar

New quantifiers based on information theory have been recently developed within a wavelet framework and applied to the characterization of brain electrical signals (see [8] and references therein), erythrocytes deformation [9], laser propagation throughout turbulent media [10,11], pseudorandom number generators [12], and quantum-classical limit [13,14]. The quantifiers are evaluated based on the time-frequency decomposition of the signal (time series) under study by recourse to the orthogonal discrete wavelet transform (ODWT) [15–17]. The ODWT makes no assumptions about the record's stationarity. In particular, if the entropy is computed via the wavelet transform, the time evolution of frequency patterns can be followed with optimal time-frequency resolution. The only input needed is the time series itself. The ensuing Shannon entropy-form, based on the wavelet transform, is called the *wavelet Shannon entropy*. It quantifies the degree of order associated with a multi-frequency signal response. Similarly, the *wavelet statistical complexity* provides us with a measure that quantifies aspects of the intricate structures hidden in the system dynamics. In this way, thermodynamics' tools inherit all the important advantages of wavelet analysis.

In the present work we characterize Gaussian self-similar stochastic processes via these wavelet-based informational quantifiers: wavelet entropy and wavelet statistical complexity. The two stochastic processes mentioned, FBM and FGN, will be used to test the performance of the above-mentioned wavelet quantifiers. In particular, from these stochastic processes and the accompanying orthogonal discrete wavelet transform we derive a discrete time-scale probability distribution in exact analytical fashion. The wavelet-based informational tools can be evaluated by using this probability distribution and enable us to gather important information about the process under study that is otherwise inaccessible. The theoretical behavior of the mentioned quantifiers will be validated on the basis of numerical simulations.

II. ENTROPY AND STATISTICAL COMPLEXITY MEASURES

López-Ruiz, Mancini, and Calbet (LMC) have proposed a statistical complexity measure based on the notion of "disequilibrium" as a quantifier of the degree of physical structure in a time series [18]. Given a probability distribution $P=\{p_j: j=1,\ldots,N_s\}$ associated with a system's state, the LMC statistical complexity measure is given by

$$C[P] = \mathcal{Q}[P] \cdot \mathcal{H}[P], \tag{2}$$

with $\mathcal{H}[P]$ a normalized entropy and $\mathcal{Q}[P]$ a distance to the uniform-equilibrium state. This quantity reflects on the interplay between the amounts of information stored in the system and its disequilibrium. LMC used the Euclidean distance in the evaluation of the disequilibrium. Martín, Plastino, and Rosso (MPR) improved on this measure by modifying the distance-component (in the concomitant probability space). In Ref. [19], $\mathcal{Q}[P]$ is built-up using Wootters' statistical distance while $\mathcal{H}[P]$ is the normalized Shannon entropy. Thus the MPR Wootters statistical complexity is given by $C_W[P] = \mathcal{Q}_W[P] \cdot \mathcal{H}[P]$, where

$$\mathcal{Q}_W[P] = \mathcal{Q}_0^{(W)} \cdot \cos^{-1}\left[\sum_{i=1}^{N_s} p_i^{1/2}\left(\frac{1}{N_s}\right)^{1/2}\right], \tag{3}$$

with $\mathcal{Q}_0^{(W)} = 1/\cos^{-1}(N_s^{-1/2})$ and $0 \leqslant \mathcal{Q}_W \leqslant 1$. Regrettably enough, the ensuing statistical complexity measure is neither an intensive nor an extensive quantity, although it yields useful results [19]. Any natural improvement should give to this statistical measure an intensive character. In a recent contribution, Lamberti, Martín, Plastino, and Rosso [20] obtained a new statistical complexity measure that is (1) able to grasp essential details of the dynamics, (2) an intensive quantity, and (3) capable of discerning among different degrees of periodicity and chaos. For this case, called MPR Jensen-Shannon statistical complexity, one has $C_{JS}[P] = \mathcal{Q}_{JS}[P] \cdot \mathcal{H}[P]$, where

$$\mathcal{Q}_{JS}[P] = \mathcal{Q}_0^{(JS)} \cdot \left\{ S\left[\frac{(P+P_e)}{2}\right] - \frac{1}{2}S[P] - \frac{1}{2}S[P_e]\right\}, \tag{4}$$

with $\mathcal{Q}_0^{(JS)} = -\frac{1}{2}\left[\left(\frac{N_s+1}{N_s}\right) - 2\ln(2N_s) + \ln N_s\right]$, P_e the uniform probability distribution, and $0 \leqslant \mathcal{Q}_{JS} \leqslant 1$. In the above expression $S[\cdot]$ denotes the Shannon entropy [21] $S[P] = -\sum_{j=1}^{N_s} p_j \ln p_j$, and the associated disorder $\mathcal{H}$ based on this measure is $\mathcal{H}[P] = S[P]/S_{\max}$, with $S_{\max} = S[P_e] = \ln N_s$.

It should be noted that the above complexity measures *are not a trivial function of the entropy*, in the sense that for a given $\mathcal{H}$-value, there exists a range of possible statistical complexity measure values between a minimum $C_{\min}$ and a maximum $C_{\max}$ [18,22,23]. Thus evaluating the statistical complexity measure provides one with important *additional* information regarding the peculiarities of a probability distribution. A general procedure for obtaining the bounds $C_{\min}$ and $C_{\max}$ corresponding to the statistical complexity family is given by Martín, Plastino, and Rosso in [23]. In statistical mechanics one is usually interested in isolated systems characterized by an initial, arbitrary, and discrete probability distribution. Evolution towards equilibrium is to be described. At equilibrium, the distribution is the equiprobability distribution. In order to study the time evolution of the statistical complexity measure, a diagram of C versus $\mathcal{H}$ can be used (in this case, $\mathcal{H}$ can be regarded as an arrow of time) [8]. Also, this kind of diagram could be used to study the system dynamics changes dependence with the characteristic parameters [13,14,20,22,23].

From the arguments mentioned previously the Martín, Plastino, and Rosso statistical complexities, C_W and C_{JS}, are suitable "measures of correlation." In this paper, both are going to be employed as informational tools for characterization of Gaussian self-similar stochastic processes.

III. WAVELET-BASED INFORMATIONAL TOOLS: A BRIEF DESCRIPTION

Wavelet analysis is one of the most useful tools when dealing with data samples. *Any* signal can be decomposed by using a wavelet dyadic discrete family $\{\psi_{j,k}(t) = 2^{j/2}\psi(2^j t - k)\}$, with $j,k \in \mathbb{Z}$ (the set of integers), of translations (indexed by k), and scaling (indexed by j) functions based on a

function ψ: the mother wavelet [15–17]. In this work j gets a frequency meaning and k a temporal one. In the case that this family is an *orthonormal* basis for $L^2(\mathbb{R})$—the space consisting of finite-energy signals—the concept of energy becomes linked with the usual notions derived from Fourier's theory. The (wavelet) coefficients in that basis are given by $C_j(k) = \langle \mathcal{S}, \psi_{j,k} \rangle$ and the corresponding, associated energy is given by the squares $|C_j(k)|^2$. If the signal is produced via a stochastic process, such origin is attached to the wavelet coefficients. The temporal average energy at each frequency-resolution $j=-1,\ldots,-N$ is defined by [24]

$$\mathcal{E}_j = \frac{1}{N_j} \sum_k \mathsf{E}|C_j(k)|^2, \tag{5}$$

where $N_j = 2^j M$ represents the number of wavelet coefficients at resolution j and E stands for the average using some, at first, unknown probability distribution associated to the coefficients. If we know that the set $\{C_j(k)\}_k$ corresponds to a stationary process the above equation reads

$$\mathcal{E}_j = \mathsf{E}|C_j(k)|^2. \tag{6}$$

Since we are using dyadic discrete wavelets the number of coefficients decreases for the low frequency bands because, at resolution level j, this number is halved with respect to the previous one for $j+1$. Thus the above energy definition emphasizes the contribution of the low frequency bands. Summing over all the available wavelet levels j we obtain the total energy

$$\mathcal{E}_{\text{tot}} = \sum_{j=-N}^{-1} \mathcal{E}_j. \tag{7}$$

We define the *relative temporal wavelet energy* (RTWE) as

$$\pi_j = \frac{\mathcal{E}_j}{\mathcal{E}_{\text{tot}}} \tag{8}$$

that supplies us with information about the relative energies associated to the different frequency bands and enables one to learn about their relative degree of importance. Since $\Sigma_{j=-N}^{-1} \pi_j = 1$, the distribution $\Pi \equiv \{\pi_j : j=-N,\ldots,-1\}$ can be thought of as yielding the probability distribution of energies across the frequency scales. This *time-scale probability density* constitutes a suitable tool for detecting and characterizing specific phenomena in both the time and the frequency planes [8–14].

In our numerical simulations we use the orthogonal cubic spline functions as the mother wavelet. Among several alternatives the symmetric and orthogonal wavelet basis obtained from it has become a recommendable tool for representing natural signals [25,26].

A typical thermodynamic concept, the entropy, is introduced within the wavelet theory in order to highlight the underlying dynamics of the system under study. Thereby, the wavelet entropy incorporates all the advantages of wavelet analysis. We define the *wavelet Shannon entropy* as

$$S[\Pi] = -\sum_{j=-N}^{-1} \pi_j \log_2 \pi_j. \tag{9}$$

As a consequence, the associated wavelet measure of disorder, called the *normalized total wavelet entropy* (NTWS) will be

$$\mathcal{H}[\Pi] = \frac{S[\Pi]}{S_{\max}}, \tag{10}$$

where Π is the probability defined in the previous section and $S_{\max} = \log_2 N$. We employ base-2 logarithms in the entropy definition so as to take advantage of the dyadic nature of the wavelet expansion, which simplifies the entropy formulas to be used in this work. As stated, the normalized total wavelet entropy is a measure of the degree of order (disorder) of the signal [8–14].

Taking as the starting point the time-scale probability density Π together with its corresponding wavelet equiprobability distribution, $\Pi_e = \{1/N,\ldots,1/N\}$, we can evaluate the wavelet-based normalized entropy $\mathcal{H}[\Pi]$ and the so-called LMC-disequilibrium $\mathcal{Q}[\Pi]$, which measures the distance of a given probabilistic distribution to the uniform one. Adopting the functional product form given by Eq. (2) a family of *wavelet statistical complexity measures* gets defined à la López-Ruiz-Mancini-Calvet by

$$C_\nu[\Pi] = \mathcal{Q}_\nu[\Pi] \cdot \mathcal{H}[\Pi], \tag{11}$$

where the index ν can adopt the values W or JS, indicating which disequilibrium is used: Wootters or Jensen-Shannon, respectively. In the case $\nu = W$ we refer to that wavelet complexity as the wavelet Martín-Plastino-Rosso with Wootters disequilibrium (WMPR Wootters), and when $\nu = JS$ as the wavelet Martín-Plastino-Rosso with Jensen-Shannon disequilibrium (WMPR Jensen-Shannon). These two complexity quantifiers derive from the original one devised by López-Ruiz, Mancini, and Calvet. We use them because they solve almost all the problems associated with the original measure, as shown in Refs. [19,20].

IV. APPLICATION TO STOCHASTIC PROCESSES

A. Fractional Brownian motion

This is the only family of processes which is (i) Gaussian, (ii) self-similar, and (iii) endowed with stationary increments [1,2]. It has been employed as a stochastic model in different and heterogeneous scientific fields, like atmospheric turbulence [10,11], econophysics [27,28] and coastal dispersion [29,30]. The normalized family of these Gaussian processes, $\{B^H(t), t>0\}$, is the one with $B^H(0)=0$ almost surely (with probability 1), $\mathbb{E}[B^H(t)]=0$ (zero mean), and covariance

$$\mathbb{E}[B^H(t)B^H(s)] = \frac{1}{2}(t^{2H} + s^{2H} - |t-s|^{2H}), \tag{12}$$

for $s,t \in \mathbb{R}$. Here $\mathbb{E}[\cdot]$ refers to the average with Gaussian probability density. The power exponent H, commonly known as Hurst parameter or Hurst exponent ([31], Chap. 8) has a bounded range between 0 and 1. These processes ex-

hibit memory, as can be observed from Eq. (12), for any Hurst parameter but $H=1/2$, for which one recovers the classical Brownian motion. In this case successive Brownian motion increments are as likely to have the same sign as the opposite, and thus there is no correlation among them. Precisely, this Hurst parameter defines two distinct regions in the interval (0, 1). When $H>1/2$, consecutive increments tend to have the same sign ([31], Sec. 9.4) so that these processes are *persistent*. For $H<1/2$, on the other hand, consecutive increments are more likely to have opposite signs ([31], Sec. 9.4) and it is said that these are *antipersistent*. Fractional Brownian motions are continuous but nondifferentiable processes (in the classical sense). As a nonstationary process, fractional Brownian motion does not possess a spectrum defined in the usual sense; however, it is possible to define a *generalized power spectrum* of the form [32]:

$$\Phi_{B^H}(f) \propto \frac{1}{|f|^\alpha}, \tag{13}$$

with $\alpha=2H+1$ and $1<\alpha<3$. Remember that this equation does not represent a valid power spectrum in the theory of stationary processes since it yields a nonintegrable function (in the classical sense).

B. Fractional Gaussian noise

We denoted by $\{W^H(t), t>0\}$ the process derived from the increment of fractional Brownian motion, namely

$$W^H(t) = B^H(t) - B^H(t+1). \tag{14}$$

We face a stationary Gaussian process with mean zero and covariance given by

$$\rho(k) = \mathbb{E}[W^H(t)W^H(t+k)]$$
$$= \frac{1}{2}[(k+1)^{2H} - 2k^{2H} + |k-1|^{2H}], \quad k>0. \tag{15}$$

The last expression has the following asymptotic behavior as $k\to\infty$ [7]

$$\frac{\rho(k)}{H(2H-1)k^{2H-2}} \to 1. \tag{16}$$

Therefore when $H>1/2$ this correlation decays to zero so slowly that the sum $\Sigma_{k=-\infty}^{k=\infty}\rho(k)=\infty$ diverges [7]; this subfamily of processes has long-memory. On the other hand, for $H<1/2$ the correlations of the increments are summable [7], and this subfamily exhibits short-memory. Equation (16) also allows one to corroborate the assertions about the persistent or antipersistent behaviors mentioned above. Note that for $H=1/2$ all correlations at nonzero lags vanish and $\{W^{1/2}(t), t>0\}$ is *white noise*. Naturally, time series of Gaussian white noise cumulatively constitute a sample of classical Brownian motion. The power spectrum associated to fractional Gaussian noise reads

$$\Phi_{W^H}(f) \propto \frac{1}{|f|^\alpha}, \tag{17}$$

with $\alpha=2H-1$ and $-1<\alpha<1$.

C. Time-scale probability distribution

We have obtained an analytical expression for the mean wavelet energy at resolution level j and time sample k for the two stochastic processes detailed above:

$$\mathbb{E}|C_j^\alpha(k)|^2 = 2c_H^2 2^{-j\alpha}\int_0^\infty \nu^{-\alpha}|\Psi(\nu)|^2 d\nu, \tag{18}$$

where $-1<\alpha<1$ (fractional Gaussian noise) or $1<\alpha<3$ (fractional Brownian motion), and c_H is calculated from the value of α. See Appendix A for further details about this result. Notice that it is independent of k, and thus stationary. Therefore the relative temporal wavelet energy is obtained replacing the above expression in Eqs. (6)–(8), that is

$$\pi_j = 2^{-(j+1)\alpha}\frac{1-2^\alpha}{1-2^{N\alpha}}, \tag{19}$$

with $-1<\alpha<3$. By continuity we have added the value $\alpha=1$, it corresponds to a constant Gaussian process (almost surely) [[6], p. 3]. In the following we will use this power-law behavior, with different α's for the two stochastic processes under analysis, unifying both into a single framework. According to its possible values, the coefficient α can be attached to one or the other of the two processes.

D. Remarks on the effects of the time-scale probability density

It is important to understand the effect that the transformation defined by Eq. (5) has in this approach. As a starting point, we have a continuous stochastic process—the signal $\mathcal{S}$—defined on the real line, which is associated to a continuous probability distribution. This transformation maps it to a *discrete process*, a random variable, whose probability is defined by Eq. (8). Obviously, because of the sampling only a finite set of resolution levels are available, so in a pragmatical sense we get a *finite* time-scale probability Π. The resulting process thus has a finite range. On the other hand, knowing all the information of the process, i.e., all the details, produces a countable (infinite) distribution, with $\mathbb{N}$ as the support set.

This mapping can be of interest for many physical applications. Also the informational tools here derived—entropies, complexity measures, etc.—exhibit rather different properties vis-a-vis those of their continuous counterparts. We refer to Pérez *et al.* [33] for details about these properties. We have also shown that, assuming an ideal infinite resolution ($N\to\infty$), the stochastic processes analyzed here (FBM and FGN) are mapped to a geometrically distributed random variable.

V. SIMULATIONS AND RESULTS

We study the performance of the wavelet-based informational tools described above and obtain the exact analytical expression associated to these quantifiers for the two families of stochastic processes described in detail in Sec. IV. In order to evaluate the normalized total wavelet entropy and wavelet statistical complexity measures, the relative wavelet energy for a finite data sample given by Eq. (19) is used. Accord-

ingly, a close form for the normalized total wavelet entropy is easily derived from Eq. (10) [34]

$$\mathcal{H}[\Pi] = \mathcal{H}(N,\alpha) = \frac{\alpha}{\log_2 N}\left(\frac{1}{1-2^{-\alpha}} - \frac{N}{1-2^{-N\alpha}}\right) - \frac{1}{\log_2 N}\log_2\left(\frac{1-2^{\alpha}}{1-2^{N\alpha}}\right). \quad (20)$$

Now, using this entropy we can obtain the WMPR Wootters and WMPR Jensen-Shannon complexities, Eq. (11), from their associated disequilibria:

$$\mathcal{Q}_W[\Pi] = \mathcal{Q}_W(N,\alpha) = \frac{1}{\cos^{-1}(N^{-1/2})}\cos^{-1}\left[N^{-1/2}\left(\frac{1-2^{-\alpha}}{1-2^{-\alpha N}}\right)^{1/2} \times \left(\frac{1-2^{-\alpha N/2}}{1-2^{-\alpha/2}}\right)\right] \quad (21)$$

and

$$\mathcal{Q}_{JS}[\Pi] = \mathcal{Q}_{JS}(N,\alpha) = -\frac{1}{\log_2 N}\sum_{j=-N}^{-1}(\pi_j + 1/N)\log_2(\pi_j + 1/N) + \mathcal{H}[\Pi] + \frac{2}{\log_2 N} - 1. \quad (22)$$

Notice that these analytical expressions for wavelet quantifiers do not depend only on the parameter α. A functional dependence with the number of wavelet levels N considered also exists.

In order to validate the previous analytical result we compare them with numerical simulations. In relation to simulation processes, Coeurjolly [35,36] has evaluated several algorithms to simulate fractional Brownian motion. From such a study we adopted the Davies-Harte algorithm [37], improved recently by Wood and Chan [38], which is both exact and fast. Actually, this method simulates fractional Gaussian noise and gets samples of fractional Brownian motion by evaluating cumulated sums of the sequential data points obtained and by setting $B_H(0)=0$. For each value of $\alpha \neq 1$ within the interval $[-0.8, 2.8]$ with step 0.2 we simulated 50 realizations with $M=5000$ *data* points in each time series. Note that for $\alpha=1$ (the limit between processes and noises) we do not have a simulation. For each set we estimate the average and mean (1) normalized total wavelet entropy and (2) wavelet statistical complexity quantifiers by using time windows of length $L=512$ *data*. See Appendix B for details about these two—average and mean—independent approaches to obtain quantifiers for the whole time series. The record length $M=5000$ *data* was chosen according to the value discussed in previous works [10,11,34]. However, when this M value is increased and the wavelet quantifiers are estimated for the same values ($N=9$ and $L=512$ *data*) the agreement between theoretical behavior and simulations results increases.

Figure 1 compares the analytical expression for the normalized entropy, Eq. (20) for $N=9$ ($j=-9,\ldots,-1$), against the estimated temporal average, $\langle\mathcal{H}\rangle$, and mean, $\tilde{\mathcal{H}}$ (normalized total wavelet entropy). Figure 2 shows estimated wavelet statistical complexity measures $\langle C_W\rangle$ and $\tilde{C}_W$ together with their theoretical expressions, also for $N=9$. Similarly, Fig. 3 depicts values for C_{JS}. It is clear from Figs. 1–3 that mean values give better results than their temporal average counterparts.

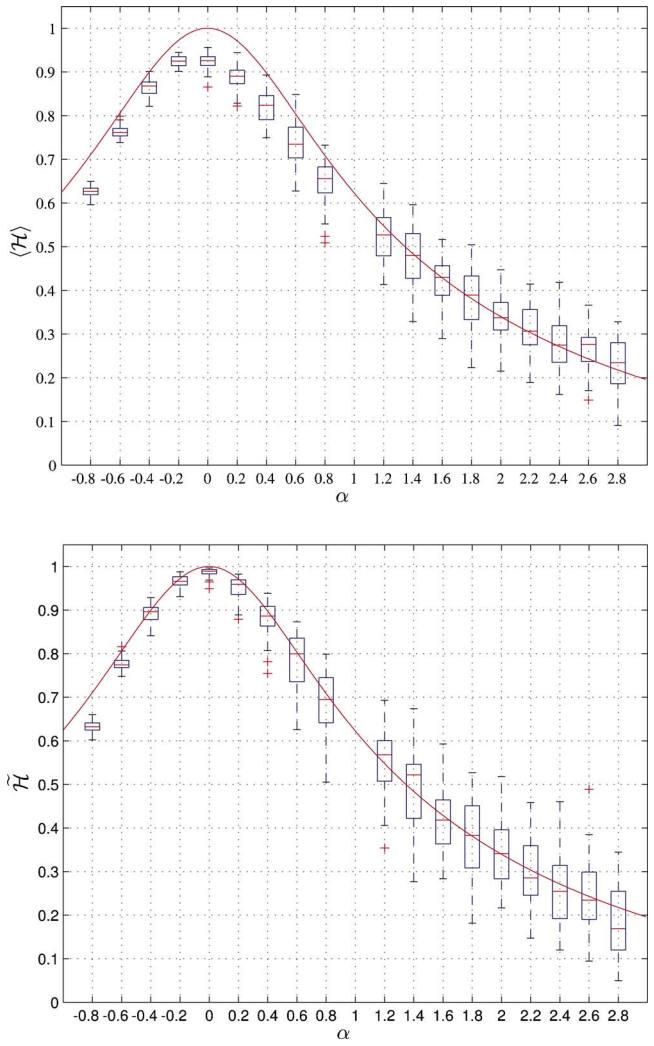

FIG. 1. (Color online) Comparison between analytical expressions—continuous line—for NTWS with $N=9$, Eq. (20), and estimated temporal average $\langle\mathcal{H}\rangle$ (top) and mean $\tilde{\mathcal{H}}$ (bottom) NTWS for FGN, $-1<\alpha<1$, and FBM, $1<\alpha<3$. Boxplots are obtained from 50 independent realizations with $M=5000$ data points each for a given α. The temporal window length was $L=512$ data points. Outliers are marked by plus signs.

Note that theoretical curves, for both wavelet quantifiers, normalized total wavelet entropy and wavelet statistical complexity measures are symmetric with respect to $\alpha=0$. In particular, for $\alpha=0$ (white noise) we have $\mathcal{H}=1$ and $C_\nu=0$ ($\nu=W,JS$), which is consistent with the hypothesis advanced in Sec. III. By inspection of Figs. 2 and 3 we conclude that wavelet statistical complexity measures exhibit a maximum value in the neighborhood of the transition point between fractional Gaussian noise and fractional Brownian motion given ($\alpha=1$). As usual, boxplots [39] illustrate lower and upper lines at the lower quartile (25th percentile of the

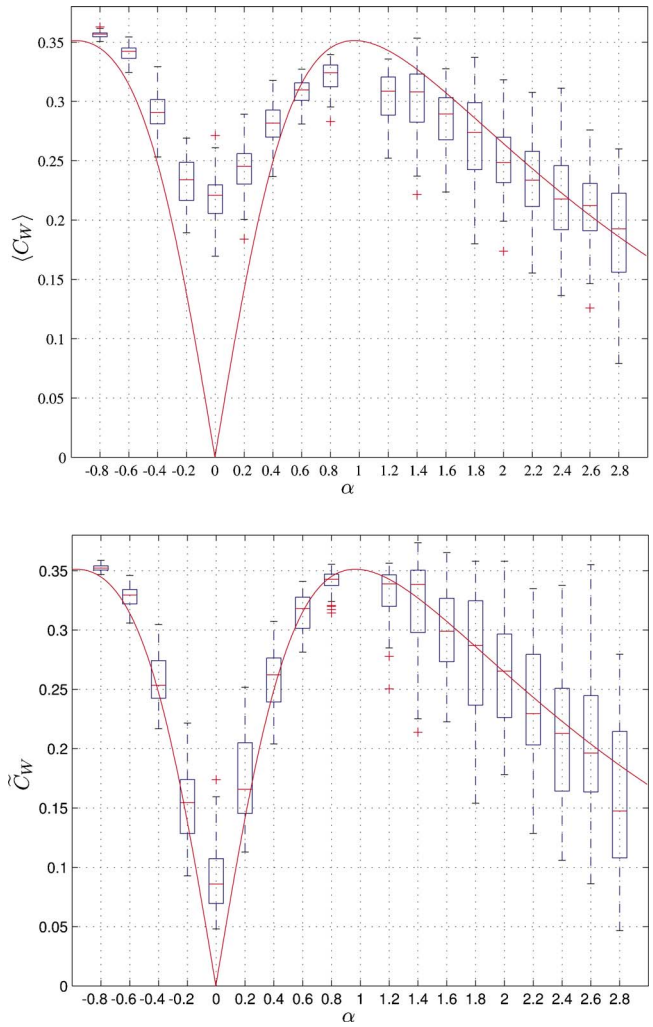

FIG. 2. (Color online) The estimated and analytical results for the MPR Wootters complexity with $N=9$—continuous line. Temporal average $\langle C_W \rangle$ (top) and mean $\widetilde{C}_W$ (bottom) WSCM for FGN, $-1<\alpha<1$, and FBM, $1<\alpha<3$. Boxplots are obtained from 50 independent realizations with $M=5000$ data points each for the given α. The temporal window length was $L=512$ data points. Outliers are marked by a plus sign.

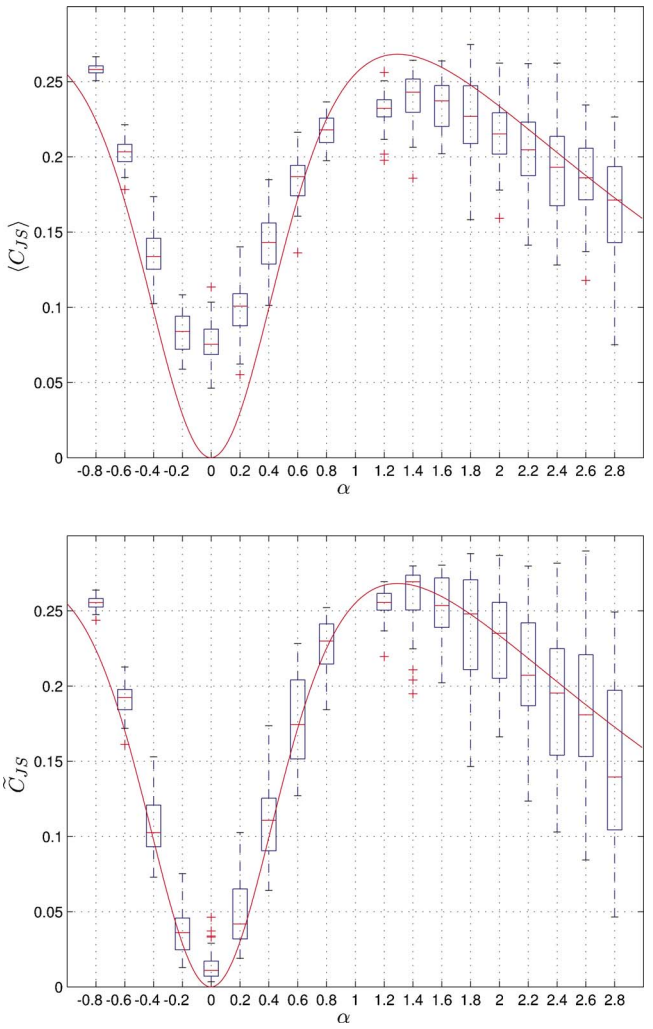

FIG. 3. (Color online) Same as Fig. 2 but for the MPR Jensen-Shannon complexity. The estimated and analytical results for the WSCM with $N=9$—continuous line. Temporal average $\langle C_{JS} \rangle$ (top) and mean $\widetilde{C}_{JS}$ (bottom) WSCM.

sample) and upper quartile (75th percentile of the sample), respectively, while the line in the middle of the box is the sample median. The whiskers are lines extending from each end of the box indicating the extent of the rest of the sample. Outliers are marked by plus signs. These points may be considered the result of either a data entry error or a poor measurement.

Finally, Fig. 4 depicts the $\widetilde{C}_{JS} \times \widetilde{\mathcal{H}}$ plane. A similar graph is obtained by using the mean WMPR Wootters statistical complexity measure. This graph is a parametric plot which allows one to visualize the behavior of the two stochastic processes with α as the parameter. As mentioned in Sec. II, the corresponding values are bounded by $C_{\max}$ and $C_{\min}$ curves [23] (evaluated for $N=9$). Their values are displayed in this figure using continuous lines. Only values in the interior of the region defined by these two limit curves can be numerically obtained. It should be stressed that the trajectory described by short- and long-memory fractional Gaussian noises, $-1<\alpha<0$ and $0<\alpha<1$, respectively, do overlap. This is due to the symmetric behavior around $\alpha=0$ of both informational quantifiers, $\widetilde{\mathcal{H}}$ and $\widetilde{C}_{JS}$, see Figs. 1 and 3. Also, notice that the right-side extremes of both theoretical results and the simulated values match with the white noise ($\widetilde{\mathcal{H}} \sim 1$ and $\widetilde{C}_{JS} \sim 0$) ones.

From inspection of Fig. 4 it is clear that our introduced wavelet-based informational tools are able to distinguish between the two stochastic processes under study. In particular, fractional Brownian motion is characterized by low-medium entropies (middle-left of the graph) and fractional Gaussian noise by medium-high entropic values (middle-right of the graph). That is, fractional Gaussian noise is more disordered than its corresponding stochastic process, the fractional Brownian motion. Also, fractional Gaussian noise exhibits decreasing (increasing) values of wavelet statistical complexity measures for parameters $-1<\alpha<0$ $(0<\alpha<1)$ corresponding to short-memory (long-memory). The case $\alpha=0$ corresponds to white noise and a maximum value of entropy

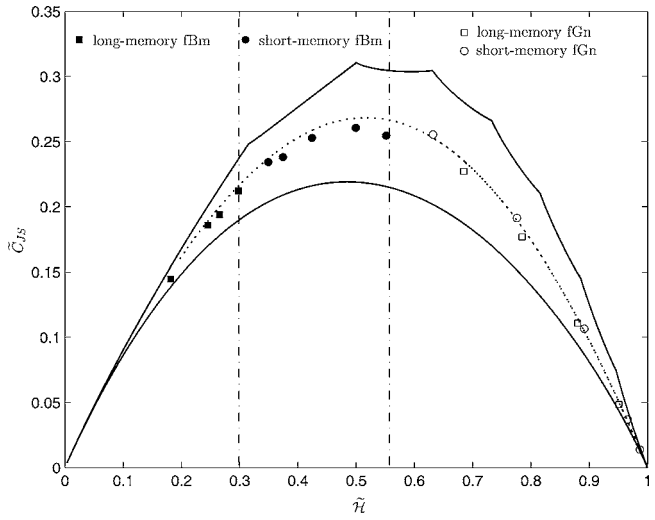

FIG. 4. $\tilde{C}_{JS}\times\tilde{\mathcal{H}}$ space for $N=9$. The parametric plot of $(\tilde{C}_{JS},\tilde{\mathcal{H}})$ in terms of the parameter α for the two stochastic processes, FBM and FGN, is shown here. The dashed line represents the theoretical expression with $N=9$. The continuous lines display the bound curves $C_{\max}$ and $C_{\min}$ associated to the maximum and minimum values of complexity for a fixed value of the normalized entropy. Vertical dash-dot lines define regions associated to the subfamilies of stochastic processes under analysis. Also, different marks are used to distinguish the numerical estimated values for these subfamilies.

together with a minimum value of complexity are jointly reached. In the case of fractional Brownian motion, wavelet-based quantifiers also distinguish between the subfamilies of short- and long-memory processes. The first, $1<\alpha<2$, is more disordered (higher entropy) and more complex than the second one, $2<\alpha<3$. Thus antipersistent processes turn out to be more complex than persistent ones. In the latter instance we are able to predict "future" behaviors. It should be noted that the two opposite extremes of complete random (white noise) and totally predictive ($\alpha\to 3$) processes have minimum complexity.

VI. CONCLUDING REMARKS

Two well-known and widely used stochastic processes, fractional Brownian motion and fractional Gaussian noise, have been characterized by using quantifiers properly defined within a wavelet framework. All the advantages of wavelet theory are therewith inherited and the initial continuous probability distribution associated with the stochastic processes under study gets mapped into a new, discrete one. Our results agree with the popular conception of maximum entropy and zero complexity for the white noise ($\alpha=0$). Noises with short- and long-memory display a symmetric behavior around this particular case. Thus they cannot be discriminated in the $C\times\mathcal{H}$ plane. However, this plane is able to discriminate the FBM processes.

As is well known, the Shannon entropy is restricted to extensive systems. For systems which have long-range correlations and fractal properties a nonextensive information measure should work better. A nonextensive entropy [40] used, for instance, in [41–45] has been shown to exhibit a good performance in describing fractal and multifractal systems. Work in progress analyzes fractal stochastic processes, like fractional Brownian motion and fractional Gaussian noise, by using this nonextensive entropy within the wavelet framework. New alternative definitions of statistical complexity measures would ensue.

ACKNOWLEDGMENTS

This work was partially supported by Consejo Nacional de Investigaciones Científicas y Técnicas (CONICET, PIP 0029/98; 5687/05 and 6036/05, Argentina), Comisión Nacional de Investigación Científica y Tecnológica (CONICYT, FONDECYT Project No. 11060512, Chile), and Pontificia Universidad Católica de Valparaíso (PUCV, Project No. 123.786/2006, Chile). D.G.P. is very grateful to Professor Mario Garavaglia for his kind hospitality at Centro de Investigaciones Ópticas (CIOp), Argentina, where part of this work was done.

APPENDIX A: TIME-SCALE PROBABILITY DISTRIBUTION. THEORETICAL RESULTS

In this appendix we revise and extend the methodology developed in Pérez *et al.* [34]. Given any Wiener space, generalized random variables $X(\omega)$, with ω one element of the statistic ensemble, can be defined through the formal sum, called *chaos expansion* [46]

$$X(\omega)=\sum_{\gamma} c_{\gamma}\mathcal{H}_{\gamma}(\omega) \quad \text{with} \quad c_{\gamma}^2=\mathbb{E}[X\mathcal{H}_{\gamma}]/\gamma!. \tag{A1}$$

Here $\gamma!=\gamma_1!\gamma_2!\cdots\gamma_n!$ is the factorial of the finite non-negative integer multiindex γ, while $\mathcal{H}_{\gamma}(\omega)=\Pi_{i=1}^{n}H_{\gamma_i}(\langle\xi_i,\omega\rangle)$ represents the stochastic component of the process, and it is built-up through the Itô integrals $\langle\xi_i,\omega\rangle$ of *Hermite functions*:

$$\xi_n(x)=\frac{e^{-x^2/2}H_{n-1}(x)}{\sqrt{2^{n-1}(n-1)!\pi^{1/2}}}, \quad n=1,2,\ldots, \tag{A2}$$

with H_n the *Hermite polynomials*. This is an orthogonal basis, and thus fulfills

$$\sum_{n=1}^{\infty}\xi_n(x)\xi_n(x')=\delta(x-x'). \tag{A3}$$

In particular, Gaussian processes attain the simplest chaos expansion, i.e.,

$$X(\omega)=\sum_{n=1}^{\infty}c_n\mathcal{H}_{\epsilon_n}(\omega), \tag{A4}$$

where $\epsilon_n=(0,0,\ldots,0,1,0,\ldots)$ with 1 on the nth entry, and 0 otherwise, so $\mathcal{H}_{\epsilon_n}(\omega)=\langle\xi_n,\omega\rangle$. Furthermore, their second moments have a simple expression through the expansion coefficients [[46], p. 43]:

$$\mathbb{E}|X|^2 = \sum_{n=1}^{\infty} |c_n|^2. \tag{A5}$$

There is a particular Wiener space for fractional Brownian processes where a stochastic calculus can be developed for the complete range of the Hurst parameter. Elliott and van der Hoek [47] were the first to introduce it, and we will use it through this section. Processes within this Wiener space are built around the self-adjoint operator M_H defined as

$$\widehat{M_H\phi}(\nu) = c_H|\nu|^{1/2-H}\hat{\phi}(\nu), \tag{A6}$$

where the hat stands for the Fourier transform, $c_H^2=\Gamma(2H+1)\sin(\pi H)$, and ϕ is any function such that $\widehat{M_H\phi} \in L^2(\mathbb{R})$. In particular, the chaos expansion for FBM results in

$$B^H(t,\omega) = \sum_{n=1}^{\infty} (M_H\mathbb{1}_{[0,t]}, \xi_n)\mathcal{H}_{\epsilon_n}(\omega), \tag{A7}$$

see Ref. [47] for further details. Since ω is fixed, whenever its presence is unnecessary it will be omitted. Since the operator M_H is self-adjoint,

$$(M_H\mathbb{1}_{[0,t]}, \xi_n) = (\mathbb{1}_{[0,t]}, M_H\xi_n) = \int_0^t ds M_H\xi_n(s).$$

Henceforth, the fractional white noise has the expansion

$$\frac{d}{dt}B^H(t) = \sum_{n=1}^{\infty} M_H\xi_n(t)\mathcal{H}_{\epsilon_n}(\omega) = W^H(t). \tag{A8}$$

Whether our signal is an FBM or FGN process their wavelet transform can be calculated accurately, but with slightly different procedures. First, let us assume that the signal is an FBM process, $\mathcal{S}(t)=B^H(t)$. Its wavelet coefficients are calculated from the orthonormal wavelet basis $\{\psi_{j,k}\}_{j,k\in\mathbb{Z}}$ as

$$C_j^{B^H}(k) = \langle B^H, \psi_{j,k}\rangle = \int_{\mathbb{R}} 2^{-j/2}\psi(2^{-j}s-k)B^H(s)ds$$
$$\overset{d}{=} 2^{(1/2+H)j}\int_{\mathbb{R}} \psi(s)B^H(s+k)ds, \tag{A9}$$

for the last step we used the self-similar property of FBM, Eq. (1). Hence, using the chaos expansion Eq. (A7) we obtain an expansion for its wavelet coefficient

$$C_j^{B^H}(k) = \sum_{n=1}^{\infty} d_n^{B^H}(j,k)\mathcal{H}_{\epsilon_n}(\omega) \tag{A10}$$

and

$$d_n^{B^H}(j,k) = 2^{(1/2+H)j}\int_{\mathbb{R}} \langle M_H\mathbb{1}_{[0,s+k]}, \xi_n\rangle\psi(s)ds. \tag{A11}$$

The evaluation of the coefficients $d_n^{B^H}(j,k)$ follows from definition (A6) and the fact that $\int_{\mathbb{R}}\psi(t)=0$:

$$d_n^{B^H}(j,k) = -c_H i^{-n}2^{(1/2+H)j}\int_{\mathbb{R}} \operatorname{sgn}\nu|\nu|^{-(1/2+H)}\Psi(\nu)$$
$$\times \xi_n(\nu)e^{-ik\nu}d\nu, \tag{A12}$$

where $\operatorname{sgn}(\cdot)$ is the sign function and $\Psi(\nu)=\hat{\psi}(\nu)$. Now, from the second moment expansion for Gaussian variables, Eq. (A5), and the orthogonality of the Hermite functions, Eq. (A3), we have

$$\mathbb{E}|C_j^{B^H}(k)|^2 = c_H^2 2^{(1+2H)j}\int_{\mathbb{R}} |\nu|^{-(1+2H)}|\Psi(\nu)|^2 d\nu$$
$$= 2\Gamma(2H+1)\sin(\pi H)2^{(1+2H)j}$$
$$\times \int_0^{\infty} \nu^{-(1+2H)}|\Psi(\nu)|^2 d\nu. \tag{A13}$$

On the other hand, if the signal is a fractional white noise, $\mathcal{S}(t)=W^H(t)$, the expansion for the coefficients is just

$$C_j^{W^H}(k) = \langle W^H, \psi_{j,k}\rangle = \sum_{n=1}^{\infty} \langle M_H\xi_n, \psi_{j,k}\rangle\mathcal{H}_{\epsilon_n}(\omega); \tag{A14}$$

and thus we are free to work with the individual coefficients

$$d_n^{W^H}(j,k) = \langle M_H\xi_n, \psi_{j,k}\rangle = c_H\int_{\mathbb{R}} |\nu|^{1/2-H}\hat{\xi}_n(\nu)\hat{\psi}_{j,k}(\nu)d\nu, \tag{A15}$$

since the Fourier transforms of the Hermite functions and the wavelet are $\hat{\xi}_n(\nu)=i^{1-n}\xi_n(\nu)$ and $\hat{\psi}_{j,k}(\nu)=2^{-j}\times\exp(-i2^{-j}k\nu)\hat{\psi}(2^{-j}\nu)$, respectively. The evaluation of the coefficients $d_n^{W^H}(j,k)$ is straightforward:

$$d_n^{W^H}(j,k) = c_H i^{1-n}2^{-(H-1/2)j}\int_{\mathbb{R}} |\nu|^{1/2-H}\Psi(\nu)\xi_n(2^j\nu)e^{-ik\nu}d\nu. \tag{A16}$$

Again, using Eq. (A5) and the orthogonality expressed in Eq. (A3) we obtain the fractional white noise's second moment

$$\mathbb{E}|C_j^{W^H}(k)|^2 = c_H^2 2^{-j(2H-1)}\int_{\mathbb{R}} |\nu|^{-(2H-1)}|\Psi(\nu)|^2 d\nu$$
$$= 2\Gamma(2H+1)\sin(\pi H)2^{-j(2H-1)}$$
$$\times \int_0^{\infty} \nu^{-(2H-1)}|\Psi(\nu)|^2 d\nu, \tag{A17}$$

for any Ψ decaying fast enough. Finally, these two expressions, i.e., Eqs. (A13) and (A17), can be combined into the one simple expression Eq. (18) written in terms of the power α.

APPENDIX B: TIME EVOLUTION

When a realization of the signal $\mathcal{S}(t)$ is sampled, as detailed in Sec. III, a finite data series results. There are two strategies to obtain the wavelet quantifiers discussed so far;

that is, the relative temporal wavelet energy, the normalized total wavelet entropy, and the wavelet statistical complexity measures. From the M data points of the sampled signal it is possible to obtain only $N=\log_2 M$ resolution levels, and at each one of these levels there will be $2^j M$ wavelet coefficients. Now, subdividing the data series into nonoverlapping (temporal) windows of length L ($i=1,\ldots,N_T$, with $N_T=M/L$) will also divide the wavelet coefficients series into N_T sets. The minimum length of the temporal window should include at least one wavelet coefficient at each level, and so $j=-N_L,\ldots,-1$, for $N_L=\log_2 L$. Now, for each interval i the different quantifiers are evaluated as follows. The wavelet energy at resolution level j for the time window i is given by

$$\hat{\mathcal{E}}_j^{(i)} = \frac{1}{N_j^{(i)}} \sum_{k=(i-1)\cdot L+1}^{i\cdot L} \mathsf{E}|C_j(k)|^2 \quad \text{with} \quad i=1,\ldots,N_T, \tag{B1}$$

and $N_j^{(i)}$ represents the number of wavelet coefficients at resolution level j corresponding to the time window i. Now, the total energy in this time window is $\hat{\mathcal{E}}_{tot}^{(i)}=\Sigma_{j<0}\hat{\mathcal{E}}_j^{(i)}$. Observe that as the process $\{C_j(k)\}$ results in being stationary the latter equation is an unbiased estimator of the temporal average energy defined in Eq. (6).

Therefore we define local versions, for the window i, of the wavelet quantifiers: the relative temporal wavelet energy at resolution level j

$$\hat{\pi}_j^{(i)} = \frac{\hat{\mathcal{E}}_j^{(i)}}{\hat{\mathcal{E}}_{\text{tot}}^{(i)}} \tag{B2}$$

gives the local time-scale probability density $\hat{\Pi}^{(i)}\equiv\{\hat{\pi}_j^{(i)}: i=1,\ldots,N_T\}$, the generalized disorder (NTWS)

$$\mathcal{H}^{(i)} = \mathcal{H}[\hat{\Pi}^{(i)}] = -\frac{1}{\log_2 N_L} \sum_{j=-N_L}^{-1} \hat{\pi}_j^{(i)} \log_2 \hat{\pi}_j^{(i)}, \tag{B3}$$

and the family of wavelet statistical complexity measures (WSCM)

$$C_\nu^{(i)} = C_\nu[\hat{\Pi}^{(i)}] = \mathcal{Q}_\nu[\hat{\Pi}^{(i)}]\cdot\mathcal{H}[\hat{\Pi}^{(i)}], \tag{B4}$$

with $\nu=W$ or JS.

Now, in order to obtain quantifiers for the full time series two independent paths can be followed. We can just average each one of the quantities above; that is, take the temporal average of normalized total wavelet entropy

$$\langle\mathcal{H}\rangle = \frac{1}{N_T}\sum_{i=1}^{N_T}\mathcal{H}^{(i)}, \tag{B5}$$

and the wavelet statistical complexity measures

$$\langle C_\nu\rangle = \frac{1}{N_T}\sum_{i=1}^{N_T} C_\nu^{(i)}. \tag{B6}$$

Also, we can take the average of the wavelet energy at resolution level j,

$$\langle\mathcal{E}_j\rangle = \frac{1}{N_T}\sum_{i=1}^{N_T}\hat{\mathcal{E}}_j^{(i)}, \tag{B7}$$

with $j=-1,\ldots,-N_L$, and also an averaged total wavelet energy $\langle\mathcal{E}_{\text{tot}}\rangle=\Sigma_{j=-N_L}^{-1}\langle\mathcal{E}_j\rangle$. In this way we are able to define a new probability distribution $\tilde{\Pi}\equiv\{\tilde{\pi}_j: j=-1,\ldots,-N_L\}$ where

$$\tilde{\pi}_j = \frac{\langle\mathcal{E}_j\rangle}{\langle\mathcal{E}_{\text{tot}}\rangle}, \tag{B8}$$

and again $\Sigma_{j=-N_L}^{-1}\tilde{\pi}_j=1$: the *mean relative temporal wavelet energy*. With respect to this new probability distribution $\tilde{\Pi}$ we define the *mean normalized total wavelet entropy*

$$\tilde{\mathcal{H}} = \mathcal{H}[\tilde{\Pi}] = -\frac{1}{\log_2 N_L}\sum_{j=-N_L}^{-1}\tilde{\pi}_j\log_2\tilde{\pi}_j, \tag{B9}$$

and the following wavelet statistical complexity measures

$$\tilde{C}_\nu = C_\nu[\tilde{\Pi}] = \mathcal{Q}_\nu[\tilde{\Pi}]\cdot\mathcal{H}[\tilde{\Pi}] \tag{B10}$$

with $\nu=W$ or JS.

[1] B. B. Mandelbrot and J. W. Van Ness, SIAM Rev. **4**, 422 (1968).

[2] G. Samorodnitsky and M. S. Taqqu, *Stable Non-Gaussian Random Processes: Stochastic Models with Infinite Variance* (Chapman and Hall/CRC, London, U.K., 1994).

[3] A. Papoulis, *Probability, Random Variables, and Stochastic Processes* (McGraw-Hill, New York, 1991).

[4] J. Lamperti, Trans. Am. Math. Soc. **104**, 62 (1962).

[5] W. Vervaat, Properties of General Self-Similar Processes, Bull. Internat. Statist. Inst. **52** (Book 4), 199–216 (1987).

[6] P. Embrechts and M. Maejima, *Selfsimilar Processes* (Princeton University Press, Princeton, NJ, 2002).

[7] J. Beran, in *Monographs on Statistics and Applied Probability* (Chapman and Hall, London, 1994), Vol. 61.

[8] O. A. Rosso, M. T. Martin, A. Figliola, K. Keller, and A. Plastino, J. Neurosci. Methods **153**, 163 (2006).

[9] A. M. Korol, R. J. Rasia, and O. A. Rosso, Physica A **375**, 257 (2007).

[10] L. Zunino, D. G. Pérez, M. Garavaglia, and O. A. Rosso, Fractals **12**, 223 (2004).

[11] L. Zunino, D. G. Pérez, M. Garavaglia, and O. A. Rosso, Physica A **364**, 79 (2006).

[12] C. M. González, H. A. Larrondo, and O. A. Rosso, Physica A **354**, 281 (2005).

[13] A. M. Kowalski, M. T. Martín, A. Plastino, A. N. Proto, and O. A. Rosso, Phys. Lett. A **311**, 180 (2003).

[14] A. M. Kowalski, M. T. Martín, A. Plastino, and O. A. Rosso, Int. J. Mod. Phys. B **19**, 2273 (2005).

[15] I. Daubechies, *Ten Lectures on Wavelets* (SIAM, Philadelphia, 1992).
[16] S. Mallat, *A Wavelet Tour of Signal Processing* (Academic Press, New York, 1998).
[17] V. Samar, A. Bopardikar, R. Rao, and K. Swartz, Brain Lang **66**, 7 (1999).
[18] R. López-Ruiz, H. L. Mancini, and X. Calbet, Phys. Lett. A **209**, 321 (1995).
[19] M. T. Martín, A. Plastino, and O. A. Rosso, Phys. Lett. A **311**, 126 (2003).
[20] P. W. Lamberti, M. T. Martín, A. Plastino, and O. A. Rosso, Physica A **334**, 119 (2004).
[21] C. E. Shannon, Bell Syst. Tech. J. **27**, 379 (1948).
[22] X. Calbet and R. López-Ruiz, Phys. Rev. E **63**, 066116 (2001).
[23] M. T. Martín, A. Plastino, and O. A. Rosso, Physica A **369**, 439 (2006).
[24] L. Zunino, D. G. Pérez, M. Garavaglia, and O. A. Rosso, Physica A (to be published).
[25] M. Unser, IEEE Signal Process. Mag. **16**, 22 (1999).
[26] P. Thévenaz, T. Blu, and M. Unser, IEEE Trans. Med. Imaging **19**, 739 (2000).
[27] E. Bayraktar, H. Vincent Poor, and K. Ronnie Sircar, Int. J. Theor. Appl. Finance **7**, 615 (2004).
[28] A. Carbone, G. Castelli, and H. E. Stanley, Physica A **344**, 267 (2004).
[29] P. S. Addison and A. S. Ndumu, Fractals **7**, 151 (1999).
[30] B. Qu, P. S. Addison, and T. Mead Christopher, Coastal Eng. **45**, 139 (2003).
[31] J. Feder, *Fractals* (Plenum Press, New York, 1988).
[32] P. Flandrin, IEEE Trans. Inf. Theory **IT-35**, 197 (1989).
[33] D. G. Pérez, L. Zunino, and O. A. Rosso (unpublished).
[34] D. G. Pérez, L. Zunino, M. Garavaglia, and O. A. Rosso, Physica A **365**, 282 (2006).
[35] J.-F. Coeurjolly, Ph.D. thesis, Laboratoire de Modélisation et Calcul-Institut d'Informatique et Mathématiques Appliquées de Grenoble, 2000 (unpublished).
[36] J.-F. Coeurjolly, J. Stat. Software **5**, 1 (2000).
[37] R. B. Davies and D. S. Harte, Biometrika **74**, 95 (1987).
[38] A. T. A. Wood and G. Chan, J. Comput. Graph. Stat. **3**, 409 (1994).
[39] J. W. Tukey, *Exploratory Data Analysis* (Addison-Wesley, Readins, MA, 1977).
[40] C. Tsallis, J. Stat. Phys. **52**, 479 (1988).
[41] P. A. Alemany and D. H. Zanette, Phys. Rev. E **49**, R956 (1994).
[42] C. Tsallis, Fractals **3**, 541 (1995).
[43] C. Tsallis, C. Anteneodo, L. Borland, and R. Osorio, Physica A **324**, 89 (2003).
[44] H. Huang, H. Xie, and Z. Wang, Phys. Lett. A **336**, 180 (2005).
[45] L. Borland, Europhys. News **36**, 228 (2005).
[46] H. Holden, B. Øksendal, J. Ubøe, and T. Zhang, *Stochastic Partial Differential Equations: A Modeling, White Noise Functional Approach*, Probability and Its Applications (Birkhäuser, Boston, 1996).
[47] R. J. Elliott and J. van der Hoek, Math. Finance **13**, 301 (2003).